

Kinetic properties of an $\text{La}_{0.85}\text{Ba}_{0.15}\text{MnO}_3$ single crystal

This article has been downloaded from IOPscience. Please scroll down to see the full text article.

2005 J. Phys.: Condens. Matter 17 5433

(<http://iopscience.iop.org/0953-8984/17/35/010>)

View [the table of contents for this issue](#), or go to the [journal homepage](#) for more

Download details:

IP Address: 129.252.86.83

The article was downloaded on 28/05/2010 at 05:53

Please note that [terms and conditions apply](#).

Kinetic properties of an $\text{La}_{0.85}\text{Ba}_{0.15}\text{MnO}_3$ single crystal

N G Bebenin^{1,3}, R I Zainullina¹, N S Chusheva¹, V V Ustinov¹ and Ya M Mukovskii²

¹ Institute of Metal Physics, Ural Division of RAS, Kovalevskaya Str, 18, Ekaterinburg 620041, Russia

² Moscow State Steel and Alloys Institute, Leninskii prospekt, 4, Moscow 117936, Russia

E-mail: bebenin@imp.uran.ru

Received 31 March 2005, in final form 27 July 2005

Published 19 August 2005

Online at stacks.iop.org/JPhysCM/17/5433

Abstract

We report the temperature and magnetic field dependence of resistivity, Hall effect, and thermopower of an $\text{La}_{0.85}\text{Ba}_{0.15}\text{MnO}_3$ single crystal. It is found that the Fermi level lies in the energy gap and conduction is by hopping. In the ferromagnetic state the variable range hopping prevails, while in the paramagnetic state hopping between nearest neighbours dominates. The small value of the activation energy of thermopower is explained by a weak asymmetry of density of states near the Fermi energy.

1. Introduction

The lanthanum–barium manganites $\text{La}_{1-x}\text{Ba}_x\text{MnO}_3$ are known to be an example of the colossal magnetoresistance (CMR) compounds. The Curie temperature T_C of these oxides can exceed the room temperature and magnetoresistance $\Delta\rho/\rho = [\rho(H) - \rho(0)]/\rho(0)$, $\rho(H)$ being resistivity in a magnetic field H , is close to $\Delta\rho/\rho$ in the La–Sr and La–Ca manganites with the same doping level. The crystal structure of some members of the La–Ba family was studied in [1–3], magnetic excitations were investigated in [4, 5], and elastic properties of La–Ba single crystals were reported in [6].

The data on electronic transport in La–Ba crystals are incomplete. The temperature dependences of resistivity and thermopower S at $H = 0$ were published for $x \leq 0.25$ [3, 7, 8] but the effect of a magnetic field on ρ and S was explored for $x = 0.20$ and 0.25 only [7, 8]. The Hall effect measurements, which can play a key role in establishing a conductivity mechanism, were carried out solely on $\text{La}_{0.80}\text{Ba}_{0.20}\text{MnO}_3$ single crystal [7].

The purpose of this paper is to study kinetic effects in $\text{La}_{0.85}\text{Ba}_{0.15}\text{MnO}_3$ single crystal and reveal the origin of the CMR in this crystal. We report the results of measurements

³ Author to whom any correspondence should be addressed.

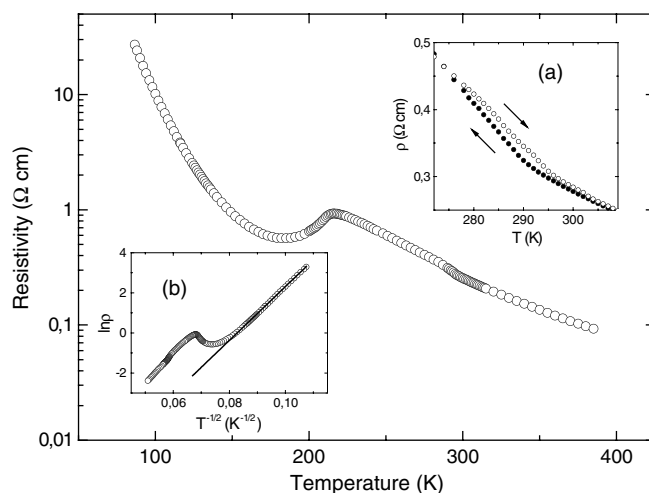


Figure 1. Temperature dependence of the resistivity of the $\text{La}_{0.85}\text{Ba}_{0.15}\text{MnO}_3$ single crystal at $H = 0$. Insets: (a) hysteresis due to the O–R transition; (b) $\ln \rho$ versus $T^{-1/2}$.

of magnetization M , resistivity, and thermopower in the temperature range 80–400 K; the Hall effect was measured at temperatures from 150 to 210 K. The magnetic field did not exceed 15 kOe. The peculiarities resulting from structural and magnetic phase transitions were explored. The focus is on the vicinity of the Curie temperature where the CMR effect is observed.

2. Experimental details

The $\text{La}_{0.85}\text{Ba}_{0.15}\text{MnO}_3$ single crystal was grown by the floating zone method. The resistivity, Hall resistivity ρ_H , and thermopower were measured using a sample in the form of a plate of size $4.5 \times 1.8 \times 0.65 \text{ mm}^3$. The magnetization measurements were performed using a vibrating sample magnetometer on a similar plate of smaller size. The resistivity was measured by a four-probe technique. The measurements of ρ and ρ_H were carried out in two opposite directions of the field and electric current. The measurements of the thermopower were made at a temperature difference of about 2 K. In all experiments, a magnetic field was perpendicular to the plane of the sample. Indium contacts were made with an ultrasonic iron.

The ordinary R_o and spontaneous R_s Hall coefficients are defined by the expression [9]

$$\rho_H = R_o B + R_s M \quad (1)$$

where B stands for the magnetic field induction inside the sample; in our case (the sample in the form of a rather thin plate) the induction may be taken to be equal to the field H . After measuring ρ_H and M , we plotted ρ_H/H versus M/H , determining thereby R_o and R_s . This method is obviously inapplicable in the paramagnetic state.

3. Results of measurements

The manganite studied is a ferromagnet. The Curie temperature evaluated through Arrott–Belov curves is 214 K, which is close to the value (218 K) reported in [3].

Figure 1 shows the temperature dependence of resistivity $\rho(T, H = 0)$ taken at heating. At all temperatures except the close vicinity of T_C the derivative $d\rho/dT < 0$, that indicates

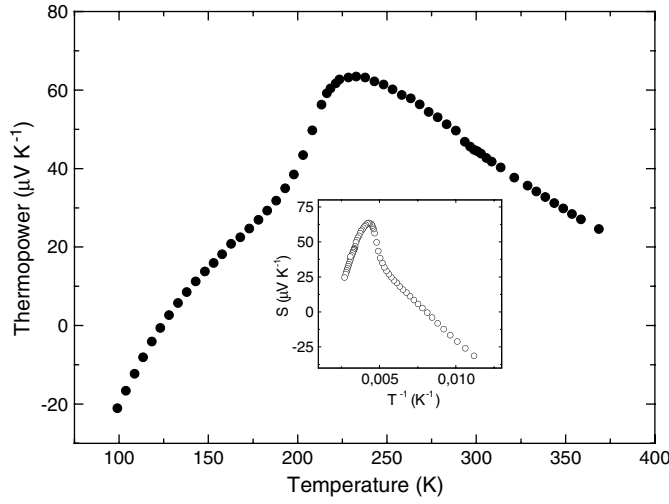


Figure 2. Temperature dependence of the thermopower at $H = 0$. Inset: S versus T^{-1} .

a conductivity of semiconductor type. Near the Curie point, the resistivity increases with T and the temperature at which $d\rho/dT$ is maximum (≈ 210 K) is close to T_C . A little below 300 K one can see a peculiarity due to the structural phase transition from the low temperature orthorhombic (O) phase to the high temperature rhombohedral (R) phase. Inset (a) in figure 1 shows the hysteresis loop connected with the O–R transition. Defining the O–R transition temperature as $T_S = (T^{\text{heat}} + T^{\text{cool}})/2$, where T^{heat} (respectively, T^{cool}) corresponds to the inflection point at the curve taken on the heating (respectively, cooling) run, we find $T_S = 284$ K. This value is somewhat higher than $T_S = 268$ K reported by Mandal and Ghosh [3] but lower than $T_S = 306$ K found in our ultrasonic experiments [6]; the variation of T_S can be ascribed to slight differences in composition.

The thermopower at $H = 0$ is plotted against temperature in figure 2. S is negative below 123 K and positive above this temperature. Below T_C , the thermopower increases with increasing T while in the paramagnetic state $dS/dT < 0$.

The effect of a magnetic field on resistivity and thermopower is shown in figure 3 where we plot $\Delta\rho/\rho$ and $\Delta S = S(0) - S(H)$ measured at $H = 10$ kOe against temperature. A magnetic field reduces both ρ and S ; the absolute values of $\Delta\rho/\rho$ and ΔS are maximum practically at the Curie point. In the paramagnetic state, see the inset in figure 3, $\Delta\rho/\rho$ and ΔS are linear in $m^2 = (M/M_s)^2$ where M_s is the saturation magnetization.

Figure 4 shows the temperature dependence of the Hall coefficients in the ferromagnetic region not far from the Curie point. Both R_0 and R_s are negative. The normal Hall coefficient depends on temperature weakly and is close to $10^{-9} \Omega \text{ cm G}^{-1}$. The spontaneous Hall coefficient is greater by an order of magnitude than R_0 and $|R_s|$ increases noticeably as T approaches T_C . Such behaviour of R_s is more or less successfully described by the formula obtained by Lyanda-Geller *et al* [10] (solid line in figure 4):

$$R_s = \rho_{xy}^{(0)} \frac{(1 - m^2)^2}{(1 + m^2)^2}, \quad (2)$$

with $\rho_{xy}^{(0)}$ being a constant.

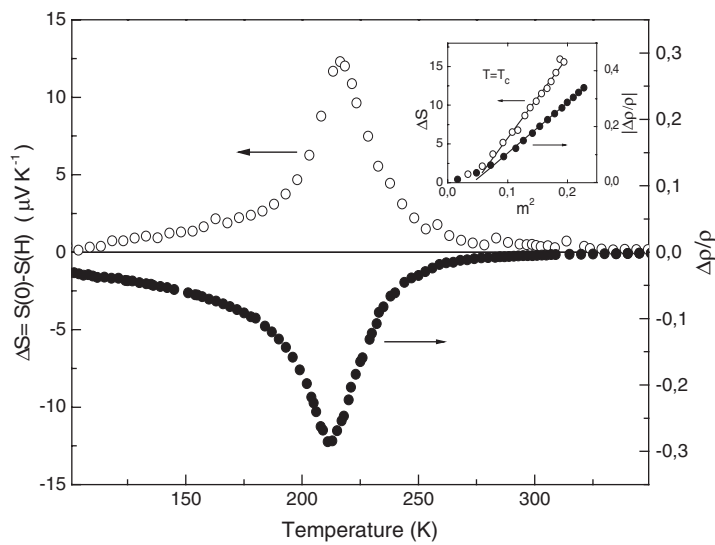


Figure 3. Effect of the magnetic field $H = 10$ kOe on the resistivity and thermopower. The inset shows $|\Delta\rho/\rho|$ and $\Delta S = S(0) - S(H)$ against squared magnetization m^2 .

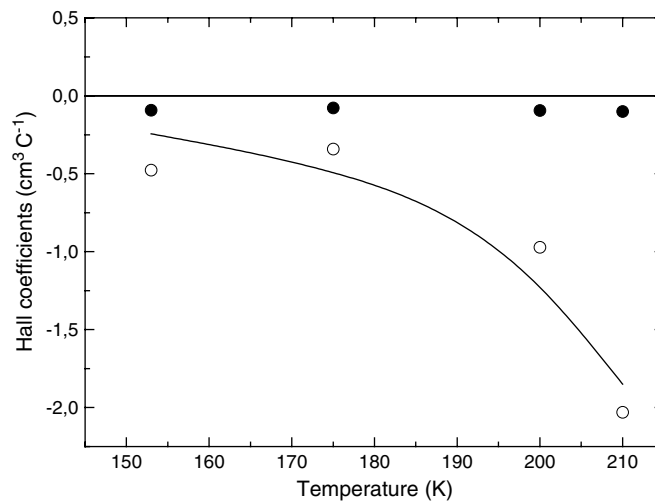


Figure 4. Normal Hall coefficient R_0 (solid circles) and spontaneous Hall coefficient R_s (open circles) versus temperature. The line is the fit to equation (2).

4. Discussion

Below 350 K, $\ln\rho$ is not a linear function of inverse temperature; therefore the activation energy for resistivity, $E_a^{(\rho)}$, depends on temperature. To understand a type of conductivity we calculated the local activation energy defined as $\varepsilon_a = d \ln \rho / d(T^{-1})$. The result is shown in figure 5. One can see the deep minimum ≈ 210 K connected obviously with the magnetic transition and the maximum at ≈ 293 K due to the structural O–R transformation. Notice that ε_a changes significantly not in a close vicinity of the Curie point but in a wide temperature range below and above T_C . Since $\varepsilon_a(T) = E_a^{(\rho)}(T) - T(dE_a^{(\rho)}/dT)$, the negative sign of

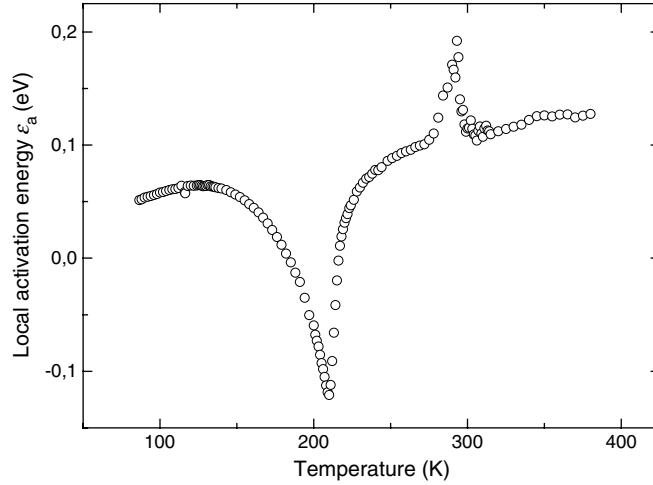


Figure 5. The local activation energy $\varepsilon_a = d \ln \rho / d(T^{-1})$ versus temperature.

ε_a points to the fast increase of $E_a^{(\rho)}$ near T_C . The width of the O–R peak is approximately equal to the width of the hysteresis loop. One can see also a weak peculiarity that occupies a narrow range from 110 to 120 K. This peculiarity is well reproduced and is not eliminated by an application of a magnetic field. Earlier [6] in an $\text{La}_{0.85}\text{Ba}_{0.15}\text{MnO}_3$ single crystal we observed the internal friction peak located at 100 K. Perhaps the weak peculiarity at the $\varepsilon_a(T)$ curve and the internal friction peak have the same origin.

Below 125 K the local activation energy increases with increasing temperature, which is an evidence for the variable range hopping (VRH). In the simplest version of VRH, the density of states (DOS) is assumed to be independent of energy near the Fermi energy E_F and the resistivity obeys the Mott law [11, 12]:

$$\rho = \rho_0 \exp[(T_0/T)^{1/4}], \quad (3)$$

where

$$T_0 = \frac{\beta}{k_B N(E_F) a^3}, \quad (4)$$

k_B stands for the Boltzmann constant, $N(E_F)$ is the DOS at $E = E_F$, a is the radius of localized states, and β is around 20. In the model by Shklovskii and Efros [12], $N(E)$ is proportional to $(E - E_F)^2$ and

$$\rho = \rho_1 \exp[(T_1/T)^{1/2}]. \quad (5)$$

The temperature dependence of ρ_0 and ρ_1 is weak and can be ignored. Our resistivity data for $T \leq 125$ K can be fitted to equation (5) (see inset (b) in figure 1) or equation (3) with practically the same accuracy. Let us first assume that the Mott law is valid. Then $T_0^{1/4} \approx 82 \text{ K}^{1/4}$, which allows us to estimate $N(E_F)$ by making use of equation (4). Although the radius of the localized states is unknown, it cannot be less than the Mn–Mn distance, so in our rough estimation we take $a = 4 \text{ \AA}$ and find that $N(E_F)$ is of order 10^{-3} states $\text{eV}^{-1} \text{ Mn}$. So the small value of $N(E_F)$ indicates the Fermi level to lie in an energy gap.

Let us estimate the width of the effective energy layer, the charge carriers of which contribute the VRH conductivity. At $T = 100$ K we obtain $\varepsilon_0 = k_B T_0^{1/4} T^{3/4} = 0.23 \text{ eV}$. This value is comparable with the energy gap, which is about 0.4 eV in pure LaMnO_3 [13];

DOS is hardly constant, even approximately, in a wide layer near E_F . The fitting to equation (5) gives $T_1^{1/2} = 133 \text{ K}^{1/2}$, then $\varepsilon_0 = k_B T_1^{1/2} T^{1/2} = 0.11 \text{ eV}$, which looks more acceptable. Thus near E_F , the density of states depends on energy essentially so that the Shklovskii–Efros model seems to be more suitable.

The calculation of DOS in a double-exchange system containing impurities [14] as well as the band calculations of electronic structure of $\text{La}_{7/8}\text{Sr}_{1/8}\text{MnO}_3$ [15] predict that the separate impurity band splits off the valence band. It is likely that the energy gap, the existence of which follows from our experiments, is the gap between the valence band and the impurity band.

Now let us turn to the thermopower. In the inset in figure 2 we plot S against inverse temperature. One can see that below 180 K the thermopower obeys the relation

$$S = \frac{k_B}{e} \left(-\frac{E_a^{(S)}}{k_B T} + A^S \right) \quad (6)$$

where $E_a^{(S)} \approx 0.011 \text{ eV}$ and $A^S \approx 1$. Notice that the first term in the parenthesis is negative as in the case of n-type conductivity, while the second term is positive. The value of $E_a^{(S)}$ is very small, being even less than $k_B T$ above 123 K. It is usually believed that if $E_a^{(S)}$ is small (significantly less than $E_a^{(\rho)}$), the charge carriers are polarons. In a hopping regime, however, such interpretation can be incorrect. Let us assume that formation of polarons does not take place. Then if the DOS is large in a restricted energy domain, e.g. narrow impurity band, $E_a^{(\rho)}$ is determined by $\int |E - E_F| N(E) dE$ while $E_a^{(S)}$ is determined roughly by $\int (E - E_F) N(E) dE$, so that $E_a^{(S)}$ is generally less than $E_a^{(\rho)}$ [16]; the values of $E_a^{(\rho)}$ and $E_a^{(S)}$ are nearly equal when the Fermi level lies well outside the impurity band. In a VRH regime, this is not the case and the thermopower can be determined by a weak asymmetry of the DOS near E_F . In accordance with the analysis of the resistivity data made above let us consider a simple model in which the DOS is given by

$$N(E) = a_0 + a_1(E - E_F) + a_2(E - E_F)^2 + a_3(E - E_F)^3 \quad (7)$$

where $a_0 = N(E_F)$ and a_2 are positive. Also assume that a_1 and a_3 , which describe the asymmetry of the DOS, are small and for simplicity (as in [16]) take the probability that a state of energy E belongs to the effective network to be independent of energy within the effective energy layer. Then

$$S = -\frac{1}{eT} \frac{\int_{E_F - \varepsilon_0}^{E_F + \varepsilon_0} (E - E_F) N(E) dE}{\int_{E_F - \varepsilon_0}^{E_F + \varepsilon_0} N(E) dE} = -\frac{1}{eT} \frac{b_1 \varepsilon_0^2 + b_3 \varepsilon_0^4}{b_0 + b_2 \varepsilon_0^2} \quad (8)$$

where b_i is proportional to a_i . If the Mott law is fulfilled $a_2 = a_3 = 0$, $\varepsilon_0 \propto T^{3/4}$ and $S \propto T^{1/2}$; when $a_0 = a_1 = 0$, we have $\varepsilon_0 \propto T^{1/2}$ and S is independent of temperature. These results are well known. Now let us assume that $\varepsilon_0 = k_B T_1^{1/2} T^{1/2}$ and $b_0 \ll b_2 \varepsilon_0^2$ (since the DOS at $E = E_F$ is very small) but $b_1 \varepsilon_0^2$ and $b_3 \varepsilon_0^4$ are of the same order. In the crystal studied, the thermopower is negative at low temperatures and changes its sign at $T = 123 \text{ K}$; consequently, $b_1 > 0$ and $b_3 < 0$. Then we obtain equation (6) with $E_a^{(S)} = b_1/b_2$ and $A^S = -b_3 T_1/b_2 > 0$. Therefore, the observed dependence of S on T is fully consistent with the VRH regime, $E_a^{(S)}$ being small due to the weakness of the asymmetry of the DOS in the vicinity of the Fermi level.

Above $T = 123 \text{ K}$, the thermopower is positive and the Hall mobility $\mu_H = R_o/\rho$ is about $-0.1 \text{ cm}^2 \text{ V}^{-1} \text{ s}^{-1}$. This μ_H value is too small for band conductivity, so the holes that conduct by hopping dominate the kinetic properties. Since S increases with T up to T_C , it is reasonable to assume that the VRH prevails in the whole ferromagnetic range.

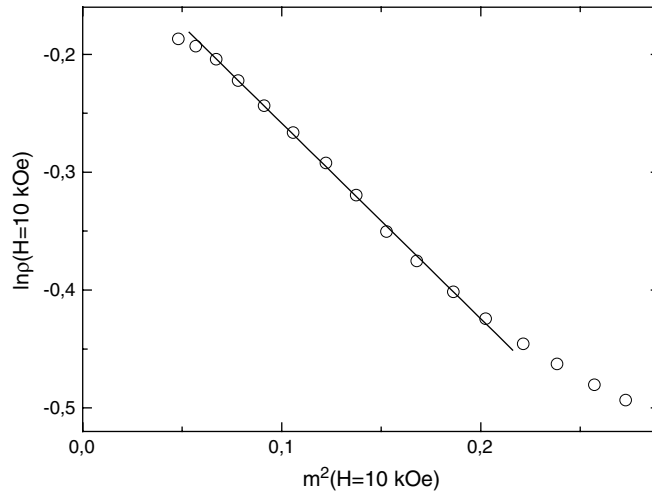


Figure 6. $\ln \rho$ against squared magnetization.

Near the Curie point, the temperature dependence of the kinetic properties is determined by the change of magnetic parameters. In figure 6 we show $\ln \rho(H = 10 \text{ kOe})$ versus squared magnetization. It is easy to see that $\ln \rho$ is linear in m^2 , therefore the growth of the resistivity near T_C results formally from the increase of the activation energy due to the increase of magnetic disorder. The same is true for the thermopower. The CPA calculations by Auslender and Kogan [17] have demonstrated that the valence and impurity bands as well as the gap between them are changed significantly as the crystal makes a transition from ferromagnetic to paramagnetic state. Therefore, the physical origin of the change of activation energies is a change of DOS accompanied by a decrease of the radius of the localized states.

The change of the local activation energy with temperature takes place also in the paramagnetic state although $m = 0$, see figure 5. This indicates that at $T > T_C$ the temperature dependence of the conductivity is controlled by spin correlation functions. As the spin correlations weaken with growing temperature, the variable range hopping is changed to the hopping between nearest neighbours, because in a double-exchange system an electron can hop from one localized state to another only if their spins are the same. The width of the effective energy layer ε_0 (and hence the activation energies of resistivity, $E_a^{(\rho)} = \varepsilon_0$, as well as that of thermopower, $E_a^{(S)}$) becomes independent of temperature. Since $E_a^{(S)}$ is determined by the asymmetrical (with respect to E_F) part of DOS, $E_a^{(S)}$ can be markedly less than $E_a^{(\rho)}$. This conclusion agrees with our experiments (see figure 5 and inset in figure 2): the activation energies for both resistivity and thermopower are independent of temperature, $E_a^{(\rho)} \approx 1500 \text{ K} = 0.14 \text{ eV}$ at $T > 350 \text{ K}$ and $E_a^{(S)} \approx 380 \text{ K} = 0.033 \text{ eV}$ at $T > 300 \text{ K}$. Notice that in our analysis we do not use the concept of polaronic transport, which is popular in the literature on the CMR manganites.

5. Conclusion

To summarize, analysis of our experimental results on electronic transport in an $\text{La}_{0.85}\text{Ba}_{0.15}\text{MnO}_3$ single crystal shows that in this crystal the Fermi level lies in the energy gap and conduction is by hopping. In the ferromagnetic state, the variable range hopping prevails. The temperature dependence of the thermopower, including the change of its sign,

can be explained by the complex structure of the density of states near the Fermi level. The positive sign of $d\rho/dT$ just below T_C results from the dependence of the activation energy on magnetization and is not evidence for a metallic regime. In the paramagnetic state hopping between nearest neighbours dominates conductivity. The asymmetry of the density of states near E_F is weak, which explains the smallness of the activation energy of the thermopower in comparison with the activation energy of the resistivity.

Acknowledgments

The work was supported by grants RFBR 03-02-16065, SS 1380.2003.2 and the Quantum Macrophysics Program.

References

- [1] Dabrowski B, Rogacki K, Xiong X, Klamut P W, Dybzinski R, Shaffer J and Jorgensen J D 1998 *Phys. Rev. B* **58** 2716
- [2] Arkhipov V E, Bebenin N G, Dyakina V P, Gaviko V S, Korolev A V, Mashkaitsan V V, Neifeld E A, Zainullina R I, Mukovskii Ya M and Shulyatev D A 2000 *Phys. Rev. B* **61** 11229
- [3] Mandal P and Ghosh B 2003 *Phys. Rev. B* **68** 014422
- [4] Arsenov A A, Bebenin N G, Gaviko V S, Mashkaitsan V V, Mukovskii Ya M, Shulyatev D A, Ustinov V V, Zainullina R I, Adams C P and Lynn J W 2002 *Phys. Status Solidi b* **189** 673
- [5] Chatterji T, Regnault L P and Schmidt W 2002 *Phys. Rev. B* **66** 214408
- [6] Zainullina R I, Bebenin N G, Burkhanov A M, Ustinov V V and Mukovskii Ya M 2005 *J. Alloys Compounds* **394** 39
- [7] Bebenin N G, Zainullina R I, Mashkaitsan V V, Gaviko V S, Ustinov V V and Mukovskii Ya M 2000 *JETP* **90** 1027
- [8] Zainullina R I, Bebenin N G, Mashkaitsan V V, Ustinov V V and Mukovskii Ya M 2003 *Phys. Solid State* **45** 1754
- [9] Hurd C M 1972 *The Hall Effect in Metals and Alloys* (New York: Plenum)
- [10] Lyanda-Geller Y, Chun S H, Salamon M B, Goldbart P M, Han P D, Tomioka Y, Asamitsu A and Tokura Y 2001 *Phys. Rev. B* **63** 184426
- [11] Mott N F and Davis E A 1979 *Electronic Processes in Non-Crystalline Materials* 2nd edn (Oxford: Clarendon)
- [12] Shklovskii B I and Efros A L 1984 *Electronic Properties of Doped Semiconductors* (Berlin: Springer)
- [13] Loshkareva N N, Sukhorukov Yu P, Mostovshchikova E V, Nomerovannaya L V, Makhnev A A, Naumov S V, Ganshina E A, Rodin I K, Moskvina A S and Balbashov A M 2002 *JETP* **94** 350
- [14] Auslender M and Kogan E 2001 *Phys. Rev. B* **65** 012408
- [15] Korotin M, Fujiwara T and Anisimov V 2000 *Phys. Rev. B* **62** 5696
- [16] Zvyagin I P 1973 *Phys. Status Solidi b* **58** 443
- [17] Auslender M and Kogan E 2001 *Eur. Phys. J.* **19** 525